In Vivo Encapsulation

DOI: 10.1002/ange.201102036

Genetically Programmed In Vivo Packaging of Protein Cargo and Its Controlled Release from Bacteriophage P22**

*Alison O'Neil, Courtney Reichhardt, Benjamin Johnson, Peter E. Prevelige, and Trevor Douglas**

Viruses have evolved exquisite selectivity for the complex hierarchical assembly of components directed towards the programmed packaging and sequestration of cargo molecules. Furthermore, protein-based containers are increasingly recognized for their ability to act as isolated intracellular compartments with unique and selective catalytic functionality.[1] The inspiration drawn from these systems has provided blueprints for synthetic encapsulation approaches based on programmed interactions in self-assembling nanocontainer systems. Heterologously expressed protein-cage architectures are excellent candidates for such engineered systems, owing to their self-assembly from a limited number of protein subunits into symmetrical, highly monodisperse structures, the ability to package or release the cargo, and the relative ease of large-scale production and purification. This approach has been used with icosahedral viral capsids to encapsulate enzymes, other proteins, and metal cores.[2,3] Furthermore, a wide range of other protein-cage architectures have been used to incorporate active sites and/or fluorescent proteins and to develop in vivo selection for packaging based on the cellular toxicity of free (unpackaged) proteases.[4]

The design of effective, widely applicable nanocontainers for programmed cargo encapsulation requires a capsid structure with sufficient internal volume for the cargo of interest to be loaded in high copy number, physical stability over a wide range of conditions, and the incorporation of molecular recognition for both specific packaging of the cargo and programmed assembly. A number of approaches have been developed for programmed encapsulation; however, in all cases the copy number of the encapsulated cargo has been relatively modest.[3,5] Herein we report an approach for the programmed encapsulation of gene-product fusions in very high copy number through the use of the capsid and scaffold-protein machinery from the bacteriophage P22 in a heterologous expression system. We used the encapsulation of a fluorescent protein as a proof of concept. Having established the methodology for genetically programmed self-assembly and encapsulation, we will be able to use the well-designed multiple cloning site described below to readily substitute a wide range of gene products into a fusion site for programmed encapsulation.

Our genetically engineered system is based on the *Salmonella typhimuriam* bacteriophage P22, which assembles from 420 copies of the coat-protein subunit into an icosahedral capsid with the assistance of 100–330 copies of a scaffold protein (SP).[6,7] The C terminus of the SP interacts with the coat protein and is necessary for self-assembly, whereas the N terminus can be severely truncated or mutated with little to no effect on assembly.[8] Our system genetically fuses cargo proteins to a truncated form of the P22 scaffold protein, which acts as a template for capsid assembly as well as a specific encapsulation signal for the cargo. In this way, additional space within the capsid from the truncation of the SP enables the cargo to be assembled in vivo with high packaging efficiency. This method does not alter the coat protein in any way. It eliminates the need for affinity tags, chemical linkers, or bridging ligands, and perhaps avoids the misassembly of virus particles. Instead, the fusion of the scaffold protein to the cargo naturally provides the necessary affinity to the interior of the capsid, and assembly is templated around the cargo.

Through genetic manipulation of the P22 assembler plasmid,[9] a vector containing the gene for P22 coat protein and a truncated variant of the wild-type (WT) scaffold protein encoding for amino acids 141–303 (SP_{141}) was designed. A thrombin-cleavage site and a new multiple cloning site (MCS) were included upstream of the SP_{141} gene. (Figure 1a; see also Figure S1 in the Supporting Information). This new MCS enabled the insertion of a series of fluorescent-protein genes (enhanced green fluorescent protein (EGFP) and mCherry[10]) for the creation of N-terminal fluorescent-protein–SP_{141} fusions. In these protein fusions, the thrombin-cleavage site is located between SP_{141} and the fluorescent protein and acts as both a flexible linker sequence and an accessible cleavage site for the release of the fluorescent protein from the SP_{141} as needed.

As expected, the P22 fluorescent-protein–SP_{141} procapsids were indistinguishable from the WT P22 procapsids during the expression and purification process except for their brilliant color, which indicated the expression, encapsulation, and proper folding of the fluorescent protein (Figure 1b). On average, the expression yields were 150 mg of P22 with encapsulated fluorescent cargo per liter of *Escherichia coli* culture after a single purification step by sucrose-cushion ultracentrifugation. Assembly of the capsids from the SP_{141}

[*] A. O'Neil, C. Reichhardt, B. Johnson, Dr. T. Douglas
Chemistry and Biochemistry Department
Center for Bio-Inspired Nanomaterials, Montana State University
Bozeman, MT 59717 (USA)
Fax: (+1) 406-994-5407
E-mail: tdouglas@chemistry.montana.edu
Dr. P. E. Prevelige
Microbiology Department, University of Alabama at Birmingham
Birmingham, AL 35294 (USA)

[**] We acknowledge the National Science Foundation (CBET-0709358) and the Department of Energy (DE-FG02-07ER46477) for financial support and thank Terje Dokland for the cryo-EM images and Prof. Steven Stowers for supplying the mCherry template DNA.

Supporting information for this article is available on the WWW under http://dx.doi.org/10.1002/anie.201102036.

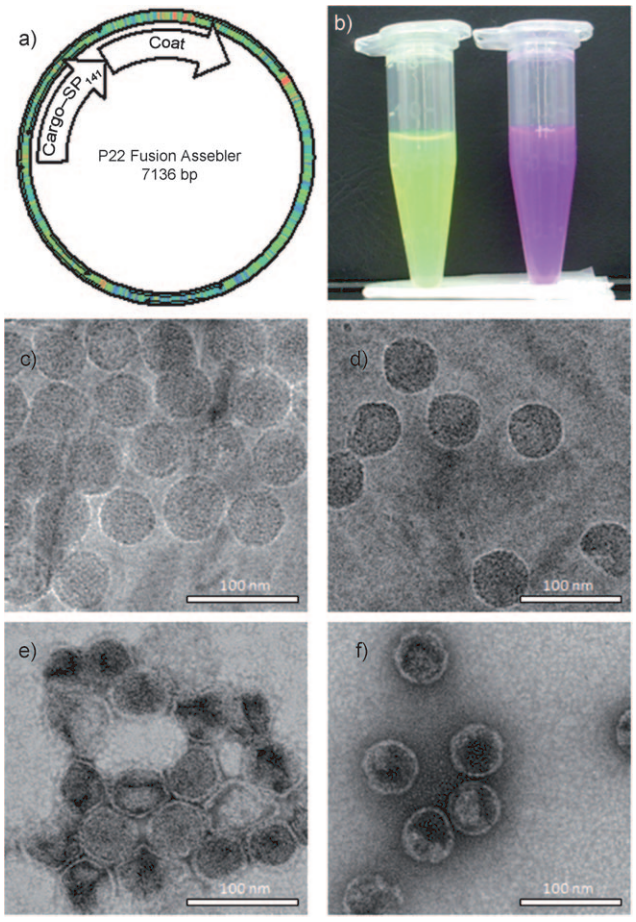

Figure 1. a) Plasmid map illustrating the gene order of the cargo–scaffold-protein fusion and the P22 coat protein. b) Purified P22 procapsids containing either EGFP–SP_{141} (left) or mCherry–SP_{141} (right). c,d) Cryo-TEM images of P22 procapsids encapsulating EGFP–SP_{141} (c) or mCherry–SP_{141} (d). e,f) Negatively stained TEM images of P22 EGFP–SP_{141} after heating to 65 °C (e) and 75 °C (f). Scale bars: 100 nm.

fusion vector was confirmed by dynamic light scattering (DLS), which yielded hydrodynamic radii, R_H, of (25 ± 2) and (24.5 ± 1.5) nm for the EGFP and mCherry constructs, and by negative-stain transmission electron microscopy (TEM), which revealed particles with radii of (22.5 ± 1) and (24.5 ± 1.5) nm for the two constructs. Additionally, cryogenic TEM (cryo-TEM) confirmed the assembly of homogeneously sized capsids with radii ranging from 24 to 25 nm for both constructs (Figure 1 c,d).

Masses corresponding to the coat protein (46 596 Da) and SP_{141} fusions (45 515 Da for EGFP–SP_{141} and 45 994 Da for mCherry–SP_{141}) were confirmed by ESIMS and by SDS-PAGE (see Figures S2 and S3). By using a preparative sephacryl S-500 size exclusion chromatography (SEC) column with the resolution to separate any aggregate from the large P22 viral capsids, we determined the visible absorbance corresponding to the fluorescent-protein fusion copurified with the capsids (see Figure S4). By HPLC size exclusion chromatography coupled to multiangle light scattering (MALS; $\lambda = 662$ nm, outside the absorption of EGFP and mCherry), we determined the diameter and total molecular weight of the constructs (see Figure S5). The determination of the molecular mass of particles in solution by MALS is based on the physical property that larger particles scatter more light. If the concentration and the dn/dc value (n = refractive index, c = concentration) of the scattering element are known, then the weight-average molecular weight (M_w) is proportional to the amount of light scattered. Particle sizes were similar to those of the nonfusion (SP_{141} only) control capsids (average R_g values (radius of gyration) were (22.5 ± 1) nm for EGFP–SP_{141}, (22.5 ± 0.8) nm for mCherry–SP_{141}, and (23.3 ± 0.3) nm for SP_{141}). Substantial mass increases were observed for the fusion-encapsulating capsids when compared to the WT P22 capsids. By MALS, the WT P22 control capsids had an average M_w value of 21.7 MDa, which increased to 32.4 MDa for EGFP–SP_{141} capsids and to 30.53 MDa for mCherry–SP_{141} capsids. On the basis of the MALS data (with an estimated 5 % error), approximately 281 EGFP and 233 mCherry fusions are contained within each P22 capsid. These results correlate well with estimates based on UV/Vis spectra (approximately 345 EGFP and 150 mCherry fusions per capsid).

It has been shown that P22 undergoes structural maturation from a spherical procapsid containing SP to an angular icosahedral mature phage of 64 nm in diameter (a 10 % increase) that lacks scaffold protein and is packed with double-stranded DNA.[6,11] This structural transition can be mimicked in vitro by gently heating the heterologously expressed procapsids to 65 °C, which expands the capsid and releases the scaffold protein. Further heating to 75 °C releases the pentamer unit from the icosahedron to create an extremely stable "wiffle ball" structure in which the shell is transected by 12 apparent 10 nm pores, but which is otherwise identical to the mature phage.[11]

The P22 SP_{141}-fusion capsids show the same temperature stability as WT P22 and undergo the same heat-induced morphological changes, which we took advantage of in the product (Figure 1 e,f; see also Figure S4 c,d). When heated to 65 °C to the expanded shell form, which lacks scaffold protein in WT P22, the scaffold-protein fusion was still constrained inside the capsid (Figure 2), as evidenced by the fluorescence signal of the fusion protein, which coeluted with the P22 capsid by SEC (S-500 column; see Figure S4). Analysis on agarose nondenaturing gel showed that the sample population of both fusions was approximately 50 % shifted to the expanded form (see Figure S6). WT P22 also showed this dual population on agarose gel when heated to 65 °C (see Figure S6). MALS analysis showed that both fusion capsids retained their cargo upon heating to 65 °C, and the M_w value decreased only slightly from 32.4 to 31.8 MDa and from 30.53 to 29.5 MDa for EGFP–SP_{141}- and mCherry–SP_{141}-containing capsids, respectively. The R_g value of the EGFP–SP_{141} capsid increased by approximately 11 % (from 22.5 to 25.2 nm), and that of the mCherry–SP_{141} capsid increased by an average of about 8.5 % (from 22.5 to 24.3 nm). Thus, the capsids underwent expansion. However, the addition of the fusion protein to SP_{141} makes it too large to escape the capsid by the normal route; this fluorescent cargo remains trapped inside the capsid during the expansion and is stable to 65 °C.

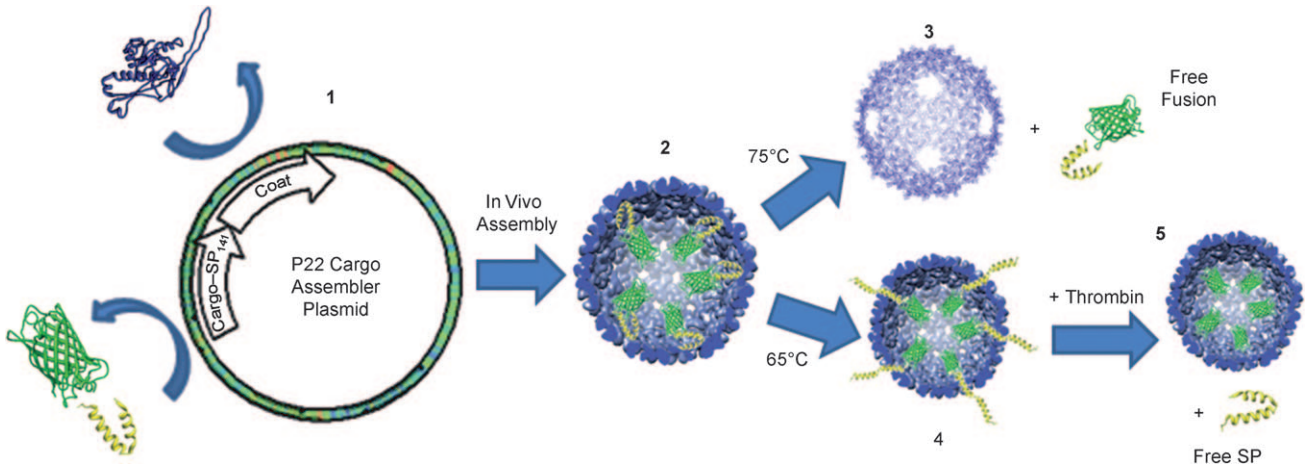

Figure 2. Illustration of the translation products from the P22 cargo assembler plasmid (coat protein and cargo–scaffold-protein fusion, 1) and how these components spontaneously assemble in vivo into a packaged P22 procapsid (2). Heating of the procapsids to 75 °C results in a wiffle-ball capsid morphology and release of the cargo (3). Heating to 65 °C leads to the expanded capsid morphology (4) and exposes the engineered thrombin site between the cargo and the scaffold protein. This site can then be cleaved to release the scaffold protein with retention of the cargo inside the capsid (5).

Upon heating to 75 °C to form the wiffle-ball structure, most of the fluorescence signal associated with the P22 capsid fraction had disappeared and was found in a later-eluting fraction by SEC (see Figure S4). This result suggests that the fluorescent cargo is free to diffuse out of the wiffle-ball form of the P22 capsid. The average M_w value of these samples was severely reduced, which suggests the capsid had lost most of the pentamer units and the encapsulated cargo (for the GFP–SP_{141} capsid, $M_w = 20.8$ MDa; for the mCherry–SP_{141} capsid, $M_w = 22.69$ MDa; the predicted M_w value of the WT P22 capsid only with no pentamers is 17 MDa). Additionally, the MALS data showed a slightly increased average radius ($R_g =$ 26.2 nm for EGFP–SP_{141} and $R_g = 25.2$ nm for mCherry–SP_{141}), which suggests the total sample population had shifted to an expanded capsid form. A nondenaturing agarose gel also confirmed the total-population morphology shift to the wiffle-ball form (Figure S6), and TEM confirmed that the capsids were intact (Figure 1 f; see also Figure S4 d). These results indicate that the capsids with internal fusions are still able to undergo the structural transition to the wiffle-ball form, and that the holes in this morphology of P22 are large enough for the SP_{141} fusion to leave the capsid.

To release the fluorescent protein cargo from SP_{141}, we first heated the fusion capsids to 65 °C to change the capsid to the expanded form, which disrupts the interaction between the scaffold protein and the capsid. The expanded fusion capsids were then treated with excess thrombin overnight. Unheated thrombin-treated samples had the same diameter and M_w as non-thrombin-treated P22 SP_{141}-fusion procapsids (for thrombin-treated EGFP–SP_{141} capsids, $M_w = 33.1$ MDa and $R_g = 22.6$ nm; for thrombin-treated mCherry–SP_{141}, $M_w =$ 31.5 MDa and $R_g = 22.5$ nm). The heated and thrombin-treated P22 SP_{141}-fusion capsids exhibited a diameter corresponding to the expanded morphology and displayed a M_w loss equivalent to the loss of SP_{141} but retention of the fluorescent protein (for heat- and thrombin-treated EGFP–SP_{141} capsids, $M_w = 29.6$ MDa and $R_g = 23.3$ nm; for heat- and thrombin-treated mCherry–SP_{141}, $M_w = 29.7$ MDa and $R_g =$ 23.5 nm). Chromatograms of the heated and thrombin-treated samples showed coelution of the fluorescence signal with the capsid and thus further illustrated the retention of the fluorescent cargo inside the capsid (see Figure S4). The release of the fluorescent protein from the scaffold protein was additionally confirmed by SDS-PAGE (see Figure S7).

In conclusion, we have demonstrated the implementation of a genetically based system for the production of a versatile nanocontainer that can direct the packaging of cargo through the use of a programmed assembly system. With our system, the in vivo encapsulation of engineered cargo in high copy number can be carried out readily and reproducibly. Furthermore, by exploiting the naturally occurring morphologies of the P22 phage, which appear to be unaffected by encapsulation of the fusion protein, we have shown the ability to control the release of the cargo from the capsid container (see Table S1 for a summary). This demonstrated control of capsid morphology may also enable directed substrate access: a necessity for encapsulated enzyme systems. The added advantage of cargo retention upon the release of the SP fusion appendage may prove useful for substrate-access issues and the oligomerization of enzymes in this system.

Through use of the designed P22–cargo assembler plasmid with introduced multiple cloning sites, it should also be possible to express and encapsulate a wide range of gene products by using the scaffold protein as both a mediator of programmed capsid assembly and a cargo-encapsulation director. The degree of control over the release of and access to cargo in either the fusion or nonfusion form makes this platform truly versatile and a promising starting point for further programmed encapsulation on the basis of genetic manipulation as the synthetic approach.

Experimental Section

To create the fusion assembler plasmid, standard PCR was used to amplify the gene for the truncated scaffold protein (AA 141-303), and 5′-NdeI and 3′-BamHI restriction enzyme recognition sequences were added, as well as a new multiple cloning site (MCS) and a thrombin-recognition site (product organization: 5′-NdeI(catatg)-SacI(gagctc)-NcoI(ccatgg)-thrombin site-SP141 gene-STOP-BamHI (ggatcc)-3′). This product was inserted to replace the full-length scaffold protein in the WT P22 assembler plasmid.[9] The gene for either EGFP or mCherry was cloned with the stop codons omitted and ligated into the new MCS, which resulted in a genetic fusion. The plasmid was transformed into XL-2Blue ultracompetent cells (Agilent Technologies, Santa Clara, CA), and colonies were screened for the presence of the insert. The confirmed-sequence fusion assembler plasmid was subsequently transformed into BL21 *E. coli* (EMD Chemicals) for protein expression.

Transformed BL21 *E. coli* were grown to $OD_{600} = 0.6$, induced with isopropyl β-D-1-thiogalactopyranoside (IPTG; 1 mM), and grown an additional 4 h. Cells were then lysed by treatment with DNase, RNase, and lysozyme (Sigma Aldrich), followed by sonication. Clarified lysates were then subjected to ultracentrifugation through a 35% (w/v) sucrose cushion. Virus pellets were resuspended in phosphate-buffered saline (pH 7.6) and further purified over a sephacryl (S-500) size exclusion column (GE Healthcare).

For HPLC–multiangle light scattering analysis, P22 capsid samples were separated by size exclusion chromatography (WTC-0200S column, Wyatt Technologies) and monitored by using both a UV/Vis detector (Agilent) and a refractive index detector (Wyatt) to determine their concentration. Multiangle light scattering was detected with a Dawn 8 instrument (Wyatt). Average M_w and R_g values were determined from a fit to the data by using a Zimm plot with the Astra software (Wyatt).

For more details, see the Supporting Information.

Received: March 22, 2011
Revised: May 16, 2011
Published online: June 28, 2011

Keywords: bacteriophages · encapsulation · fluorescent proteins · gene technology · nanocontainers

[1] a) S. Tanaka, M. R. Sawaya, T. O. Yeates, *Science* **2010**, *327*, 81; b) S. Tanaka, C. A. Kerfeld, M. R. Sawaya, F. Cai, S. Heinhorst, G. C. Cannon, T. O. Yeates, *Science* **2008**, *319*, 1083; c) S. Kang, T. Douglas, *Science* **2010**, *327*, 42.

[2] a) J. D. Fiedler, S. D. Brown, J. L. Lau, M. G. Finn, *Angew. Chem.* **2010**, *122*, 9842; *Angew. Chem. Int. Ed.* **2010**, *49*, 9648; b) I. J. Minten, V. I. Claessen, K. Blank, A. E. Rowan, R. J. M. Nolte, J. J. L. M. Cornelissen, *Chem. Sci.* **2011**, *2*, 358; c) M. Comellas-Aragonès, H. Engelkamp, V. I. Claessen, N. A. J. M. Sommerdijk, A. E. Rowan, P. C. M. Christianen, J. C. Maan, B. J. M. Verduin, J. J. L. M. Cornelissen, R. J. M. Nolte, *Nat. Nanotechnol.* **2007**, *2*, 635; d) S. Kang, M. Uchida, A. O'Neil, R. Li, P. E. Prevelige, T. Douglas, *Biomacromolecules* **2010**, *11*, 2804; e) J. Sun, C. DuFort, M.-C. Daniel, A. Murali, C. Chen, K. Gopinath, B. Stein, M. De, V. M. Rotello, A. Holzenburg, C. C. Kao, B. Dragnea, *Proc. Natl. Acad. Sci. USA* **2007**, *104*, 1354.

[3] T. Inoue, M.-a. Kawano, R.-u. Takahashi, H. Tsukamoto, T. Enomoto, T. Imai, K. Kataoka, H. Handa, *J. Biotechnol.* **2008**, *134*, 181.

[4] a) B. Worsdorfer, K. J. Woycechowsky, D. Hilvert, *Science* **2011**, *331*, 589; b) S. Kang, L. M. Oltrogge, C. C. Broomell, L. O. Liepold, P. E. Prevelige, M. Young, T. DougIas, *J. Am. Chem. Soc.* **2008**, *130*, 16527; c) M. Suzuki, M. Abe, T. Ueno, S. Abe, T. Goto, Y. Toda, T. Akita, Y. Yamadae, Y. Watanabe, *Chem. Commun.* **2009**, 4871; d) C. Jolley, M. Klem, R. Harrington, J. Parise, T. Douglas, *Nanoscale* **2011**, *3*, 1004.

[5] a) V. A. Kickhoefer, Y. Garcia, Y. Mikyas, E. Johansson, J. C. Zhou, S. Raval-Fernandes, P. Minoofar, J. I. Zink, B. Dunn, P. L. Stewart, L. H. Rome, *Proc. Natl. Acad. Sci. USA* **2005**, *102*, 4348; b) F. P. Seebeck, K. J. Woycechowsky, Z. Wei, J. P. Rabe, D. Hilvert, *J. Am. Chem. Soc.* **2006**, *128*, 4516; c) I. J. Minten, L. J. A. Hendriks, R. J. M. Nolte, J. J. L. M. Cornelissen, *J. Am. Chem. Soc.* **2009**, *131*, 17771; d) Q. Chen, H. Schönherr, G. J. Vancso, *Small* **2010**, *6*, 2762.

[6] W. Earnshaw, S. Casjens, S. C. Harrison, *J. Mol. Biol.* **1976**, *104*, 387.

[7] W. Jiang, Z. Li, Z. Zhang, M. L. Baker, P. E. Prevelige, W. Chiu, *Nat. Struct. Biol.* **2003**, *10*, 131.

[8] a) M. H. Parker, S. Casjens, P. E. Prevelige, Jr., *J. Mol. Biol.* **1998**, *281*, 69; b) P. R. Weigele, L. Sampson, D. Winn-Stapley, S. R. Casjens, *J. Mol. Biol.* **2005**, *348*, 831.

[9] P. E. Prevelige, Jr., D. Thomas, J. King, *J. Mol. Biol.* **1988**, *202*, 743.

[10] N. C. Shaner, R. E. Campbell, P. A. Steinbach, B. N. G. Giepmans, A. E. Palmer, R. Y. Tsien, *Nat. Biotechnol.* **2004**, *22*, 1567.

[11] C. M. Teschke, A. McGough, P. A. Thuman-Commike, *Biophys. J.* **2003**, *84*, 2585.

